Journal of New Technology and Materials (JNTM)
J. New Technol. Mater.
Vol. 08, N°01 (2018)114-119

OEB Univ. Publish. Co.

Optimization of a GaAsN ternary alloy based solar cell for high efficiency

K. Ameur, H. Mazari, N. Benseddik, Z. Benamara, N. Benyahya and A. Boumesjed

Laboratory of Applied Micro Electronics, Department of Electronics,
University Djillali Liabes of Sidi Bel Abbes, 22000 Sidi Bel Abbes, Algeria

Corresponding author: kheira_ameur@yahoo.fr

Received date: Jan. 20, 2018; accepted date: June 05, 2018

Abstract

We report on the photovoltaic characteristics of solar cells based on $GaAs_{1-x}N_x$ grown on gallium arsenide. The GaAsN is a recently developed novel solar cell material for its promising tunable band gap of 1.42 eV to 3.4 eV for the realization of high efficiency solar cells. We have conducted numerical simulation of $GaAs_{1-x}N_x$ single junction solar cell. The doping density, layer thickness, and the stoichiometric *coefficient are investigated for optimized performance of solar cell under solar illumination of AM1.5G. Thus starting from I-V curves, we have calculated the short-circuit current I_{cc}, the open-circuit voltage V_{oc} and the efficiency conversion. This structure can also provide a fundamental solar cell unit for developing very high efficiency MQW solar cell.*

Keywords: GaAsN; Solar cell; Conversion efficiency

1. Introduction

Today, much research is focused on increasing the efficiency of solar cells made with new materials such as III-V nitrided alloys (III-$V_{1-x}N_x$). The variation of the incorporation of nitrogen in these ternary alloys allows the considerable modification of their physical and optical properties. Generally, these new materials are deposited in thin layers, but still present interesting efficiency, thus reducing production costs.

However, optimizing the performance of the III-$V_{1-x}N_x$ optoelectronic devices requires a better understanding of the physical and optical properties of these alloys, particularly their function as solar cells. The ternary alloy $GaAs_{1-x}N_x$ is obtained by using GaAs and GaN, both of direct bandgap and respective energies 1.42 eV (near infrared) and 3.4 eV (ultraviolet) at room temperature, one could expect to form a $GaAs_{1-x}N_x$ alloy which could describe the entire spectrum of the visible according to the values of the stoichiometric coefficient x.

The synthesis of low-nitrogen GaAsN alloys became technically feasible with the appearance of plasma cells in 1990 [1,2], a strong infrared shift of absorption [2] and of photoluminescence [1,3] was observed, suggesting a decrease in gap energy of $GaAs_{1-x}N_x$ with incorporation of nitrogen. This result, although surprising, was quickly supported by theoretical work [4]. The $GaAs_{1-x}N_x$ alloy (with small values of stoichiometric coefficient x) possesses in fact a large bowing parameter. This parameter varies with the nitrogen composition. Its value is of the order of 20 to 25 eV for x < 1%, and of 15 to 20 eV for x > 1% [5,6].

The object of this paper is therefore to determine the photovoltaic parameters, in particular the conversion efficiency using a small amount of nitrogen incorporation x.

Using the PCID (version 5) software [7], we were able to simulate the photoelectric behavior of $GaAs_{1-x}N_x$ based on PN junction. This is done from the numerical simulation of the current-voltage characteristic (I-V) under the conditions of solar illumination AM1.5G [8]. Our investigation is to see the sensitivity of output photovoltaic parameters such as short-circuit current (I_{cc}), open-circuit voltage (V_{oc}) and conversion efficiency (η).

2. Description of simulated solar cell

The structure to be studied is a PN junction cell whose principle diagram is shown in figure 1. It consists mainly of an N-type layer which represents the front and another P-type layer which represents the base. The base substrate is GaAs which served as a support for the growth of $GaAs_{1-x}N_x$.

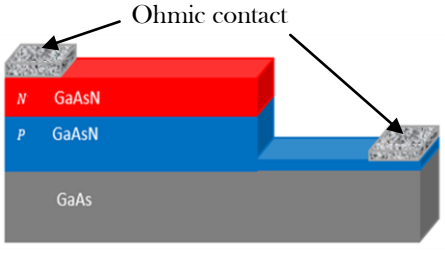

Figure 1. PN solar cell based on GaAsN.

3. Results and discussion

The optimization of the output quantities (short-circuit current, open-circuit voltage, fill factor and conversion efficiency) will depend on the technological parameters concerning the front and the base in a solar cell to PN junction, in particular thickness and doping.

The simulation was done by optimizing the output parameters by varying the physical or technological quantities for the value of x = 4%. The choice of this value is justified by the availability of its extinction coefficient [9] which is function of the absorption coefficient (α). We also simulated the I-V characteristics of the single junction PN solar cells based on cubic GaAs (α is given by [7]) and cubic GaN (α is given by [10]) in order to compare their conversion efficiency with that of the solar cell based on $GaAs_{0.96}N_{0.04}$ (x = 4%).

The studied material $GaAs_{0.96}N_{0.04}$ has a band gap energy (E_g) of 1.337 eV, this value is extracted from the experimental curve of the work of Ribeiro and al [11].

Using the linear interpolation scheme for ternary material [12], the electron affinity of GaAsN is expressed by the relation:

$$\chi(GaAs_{1-x}N_x) = (1-x)\,\chi(GaAs) + x\,\chi(GaN) \qquad (1)$$

For nitride ternary alloys, generally, the bowing of mobility is very great [13] from where the carrier mobility is given by the following expression [13]:

$$\frac{1}{\mu_{n,p}(GaAs_{1-x}N_x)} = \frac{(1-x)}{\mu_{n,p}(GaAs)} + \frac{x}{\mu_{n,p}(GaN)} \qquad (2)$$

μ_n and μ_p are the electron and hole mobility, respectively.

The relative permittivity of ternary material is given by [12]:

$$\varepsilon_r(GaAs_{1-x}N_x) = (1-x)\,\varepsilon_r(GaAs) + x\,\varepsilon_r(GaN) \qquad (3)$$

The electron and hole effective mass (m_e^*, m_t^*) used in the calculation of density of states in the conduction band (N_c), valence band (N_v) and intrinsic concentration (n_i) vary linearly as a function of x according to the relationship [12]:

$$m_{e,t}^*(GaAs_{1-x}N_x) = (1-x)\,m_{e,t}^*(GaAs) + x\,m_{e,t}^*(GaN) \qquad (4)$$

The refractive index (n) as a function of x is extracted from the curve given in the work of Biswas and al [9].

Table 1 shows the physical parameters of the $GaAs_{1-x}N_x$ for the values of x chosen and which are used in simulation.

Table 1. Specific physical parameters of $GaAs_{1-x}N_x$ for three values of x: 0 %, 4 %, and 100%.

Stoichiometric coefficient / *Physical Parameters*	x = 0% c-GaAs	x = 4% $GaAs_{0.96}N_{0.04}$	x = 100% c-GaN
Band gap E_g (eV)	1.42 [14]	1.337 [11]	3.35 [18]
Electron affinity χ (eV)	4.07 [14]	4.071	4.1 [19]
Electron mobility μ_n ($cm^2V^{-1}s^{-1}$)	8500 [14]	6538.461	1000 [20]
Hole mobility μ_p ($cm^2V^{-1}s^{-1}$)	400 [14]	397.727	350 [21}
Relative permittivity ε_r	12.5 [15]	12.388	9.7 [19]
Electron effective mass m_e^*	0.067 [16]	0.070	0.15 [13]
Hole effective mass m_t^*	0.64 [16]	0.648	0.86 [22]
Density of states in BC N_c (cm^{-3})	4.335×10^{17}	4.662×10^{17}	1.452×10^{18}
Density of states in BV N_v (cm^{-3})	1.28×10^{19}	1.306×10^{19}	1.994×10^{19}
Intrinsic concentration n_i (cm^{-3})	3.1×10^{6}	1.7×10^{7}	4.4×10^{7}
Refractive index n	3.6 [17]	2.95 [9]	2.15 [9]

In table 2, we list the specific parameters used in simulation (default values and variation range) for each region (front and base) of the PN junction solar cell.

Table 2. Specific parameter values for a $GaAs_{1-x}N_x$ PN junction cell.

Parameters	Default values	Extension of variation
Front thickness X_E (µm)	0.1	0.1 – 1
Base thickness X_B (µm)	1	0.5 – 4
Front doping N_D (cm^{-3})	10^{17}	5×10^{15} - 5×10^{17}
Base doping N_A (cm^{-3})	10^{16}	10^{15} - 10^{18}

3.1. Effect of the front technological parameters

3.1.1. Effect of the front thickness

The influence of the thickness on the output parameters for the PN solar cell based on GaAsN is shown in figure 2.

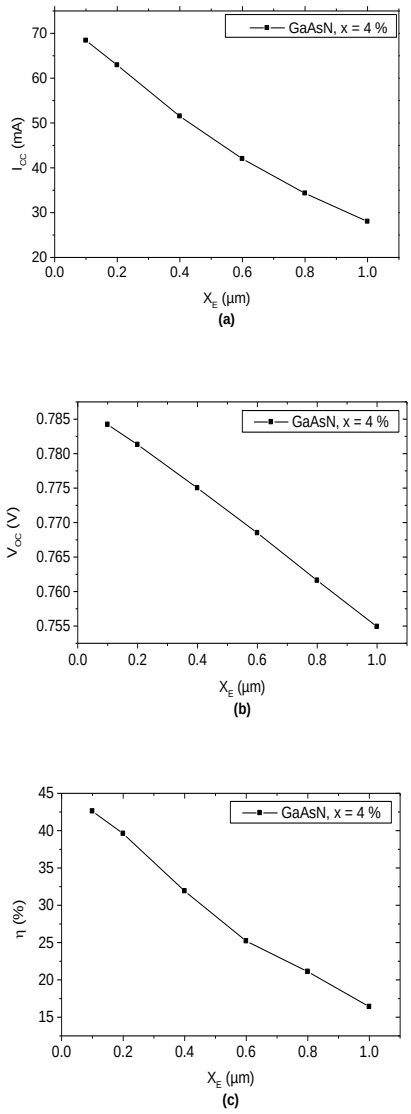

Figure 2. Variation of the photovoltaic parameters as a function of the thickness of the front for x = 4% ($GaAs_{0.96}N_{0.04}$). (a)- photocurrent I_{cc}, (b)- open-circuit voltage V_{oc}, (c)- conversion efficiency η.

From figure 2.(a), 2.(b), 2.(c), we observe that the photocurrent I_{cc}, the open-circuit voltage V_{oc} and the efficiency η decrease as the thickness of the front increases. For small thicknesses of the front the photogenerated minority carriers easily reach the depletion region and can therefore contribute to the total photocurrent. But if the thickness of the front increases, these photocarriers recombine before reaching this zone and the photocurrent decreases.

3.1.2. Effect of the front doping

The doping of the front is a very important technological parameter to optimize the photovoltaic quantities. The influence of the latter is illustrated in figure 3.

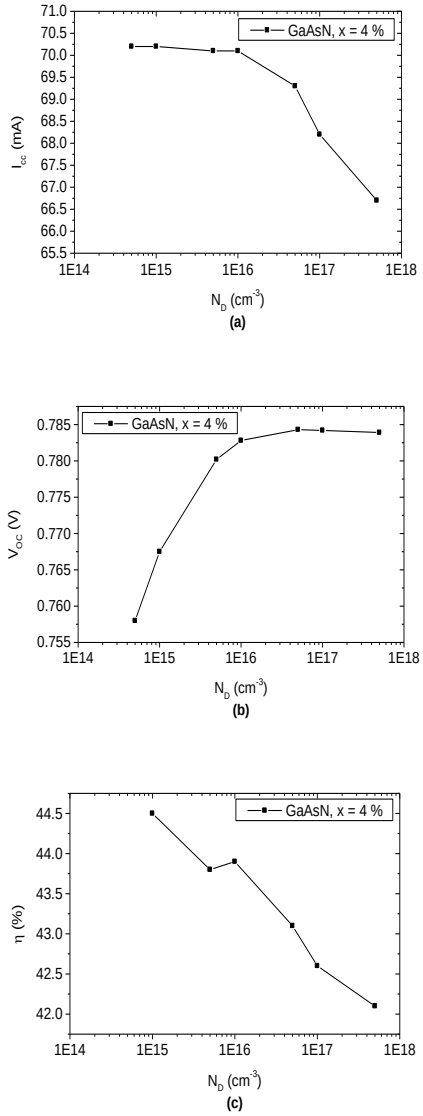

Figure 3. Variation of the photovoltaic parameters as a function of the doping of the front for x = 4% ($GaAs_{0.96}N_{0.04}$) (a)- photocurrent I_{cc}, (b)- open-circuit voltage V_{oc}, (c)- conversion efficiency η.

We note from figure 3.(a), 3.(b), 3.(c) that the photocurrent is constant up to the value of N_D in the order of 10^{16} cm^{-3}, after this value the photocurrent I_{cc} decreases. The open-circuit voltage V_{oc} increases with doping up to $N_D = 10^{16}$ cm^{-3} and then stabilizes. The efficiency η is at its maximum for a doping of the order of 10^{15} cm^{-3}, after it decreases.

Therefore, when the doping of the front (N) increases, the mobility of the carriers decreases, the semiconductor becomes degenerate, the photocurrent and the conversion efficiency decrease.

3.2. Effect of the base technological parameters

3.2.1. Effect of the base thickness

The influence of the thickness of the base on the output parameters of the PN solar cell is shown in figure 4.

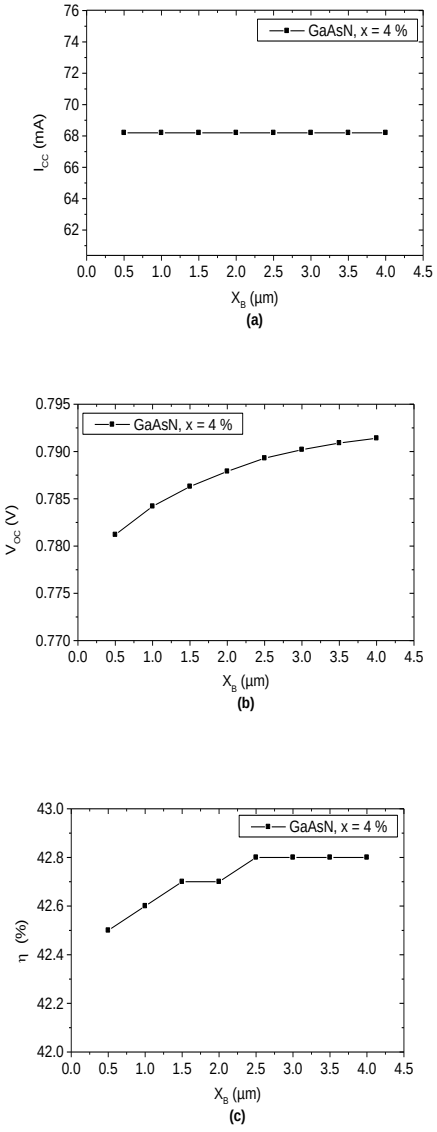

Figure 4. Variation of the photovoltaic parameters as a function of the thickness of the base for x = 4% ($GaAs_{0.96}N_{0.04}$).
(a)- photocurrent I_{cc}, (b)- open-circuit voltage V_{oc}, (c)- conversion efficiency η.

We note from figure 4.(a) that the photocurrent I_{cc} remains constant whatever the thickness of the base. The open-circuit voltage V_{oc} increases slightly with the thickness of the base (figure 4.(b)). The conversion efficiency η increases slightly to reach a constant value of 42.8% (figure 4.(c)). When the thickness of the base increases, if the diffusion length of the minority carriers (electrons) remains high compared to the thickness of the base, in this case the recombinations are negligible, so the photocurrent and the conversion efficiency remain almost constant.

3.2.2. Effect of the base doping

The influence of the base doping on the output parameters in the solar cell PN based on GaAsN is shown in figure 5.

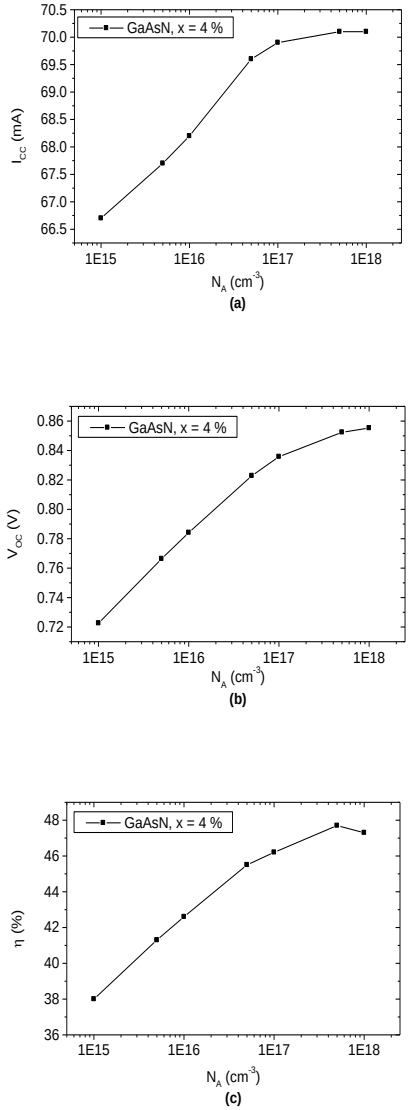

Figure 5. Variation of the photovoltaic parameters as a function of the doping of the base for x = 4% ($GaAs_{0.96}N_{0.04}$),

(a)- photocurrent I_{cc}, (b)- open-circuit voltage V_{oc}, (c)- conversion efficiency η.

The short-circuit current (figure 5.(a)), the open-circuit voltage (figure 5.(b)) and the conversion efficiency (figure 5.(c)) increase with the doping of the base until reaching maximum values. Beyond 5×10^{17} cm^{-3}, the efficiency decreases slightly.

When the doping of the base (P) increases, the electric field increases, it accelerates the passage of photogenerated minority carriers, hence the increase of the total photocurrent and subsequently the increase of the conversion efficiency.

After analyzing the results obtained by the simulation, the best technological parameters for the front and the base of a PN junction solar cell for x = 4% ($GaAs_{0.96}N_{0.04}$) are: X_E= 0.1 µm with N_D = 5×10^{16} cm^{-3}, X_B= 4 µm with N_A= 5×10^{17} cm^{-3} respectively. Using these optimized parameters, we plotted current-voltage characteristic.

Figure 6 shows the simulated current-voltage characteristics of single photovoltaic cells based on $GaAs_{1-x}N_x$ corresponding to x = 0%, x = 4% and x = 100%.

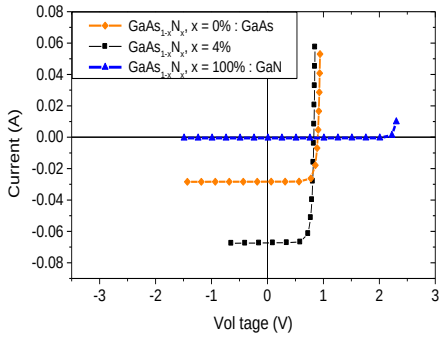

Figure 6. Current-voltage characteristics of solar cells based on $GaAs_{1-x}N_x$ for three values of x.

Table 3 groups together the output parameters of the PN junction solar cell based on the $GaAs_{1-x}N_x$ material (for an area of 1 cm^2) with three values of the stoichiometric coefficient x.

Table 3. Output parameters of PN single junction solar cell based on $GaAs_{1-x}N_x$ with the three values of x.

x (%)	0 (GaAs)	4 ($GaAs_{0.96}N_{0.04}$)	100 (GaN)
I_{cc} (mA).	28.3	67.3	0.494
V_{oc} (V)	0.8986	0.8287	2.210
η (%).	20.4	44.6	1.03

From this table, it should be noted that the $GaAs_{0.96}N_{0.04}$ cell, a low-gap material, has a significantly higher efficiency than the GaN cell, a material with a large gap.

Note that current research focuses on the small values of x because GaAsN remains difficult to synthesize, the structure exhibiting defects in the crystal structure. We present in table 4 experimental results obtained in the literature for single junction cells based on GaAsN growth by MBE [23,24] compared to single junction cells based on GaAs [25] and our results.

Table 4. Output parameters reported in the literature for single junction $GaAs_{1-x}N_x$ cells grown by MBE [23,24], compared to single junction GaAs cells [25] and our results.

Parameter / Material	x (%)	J_{cc} (mA/cm^2)	V_{oc} (V)	η (%)
GaAs [25]	0	29.6	1.107	27.6
GaAs Our results	0	28.3	0.8986	20.4
GaAsN MBE [23]	1	14.16	0.31	2.94
GaAsN MBE [24]	3.5	33	0.5	/
GaAsN Our results	4	67.3	0.8287	44.6

We have observed, after optimization of the output parameters, that a high conversion efficiency is obtained with the GaAsN solar cell having a coefficient x of 4%. This optimization was achieved with the proper choice of technological parameters. Technology is the key point leading to the realization of high efficiency solar cells.

Our results, which remain purely theoretical, have given us an idea of the high efficiency that can be achieved with advanced GaAsN material technology.

4. Conclusion

The work presented in this paper concerns the study of photovoltaic cells based on GaAsN nitrided materials. The main objective is to optimize the front and base with their thickness and doping, on the electrical characteristic of the photovoltaic cell and subsequently its output parameters.

The optimization of the solar cell based on $GaAs_{1-x}N_x$ was made for nitrogen incorporation (x) of 4%. Experimental results obtained in the literature for single junction cells based on GaAsN growth by MBE were compared to the single junction GaAs cells and to our results which remain purely theoretical but which give an indication of the high efficiency which can be obtained in case an improvement in GaAsN technology is made.

Finally, our simulation results can contribute to the study and design of multi-junction or tandem solar cells

based on the GaAsN material for space applications and terrestrial.

References

[1] M. Weyers, M. Sato, Applied Physics Letters, 62 (1993) 1396-1398.

[2] M. Sato, Journal of Crystal Growth, 145 (1994) 99-103.

[3] M. Weyers, M. Sato, H. Ando, Japanese Journal of Applied Physics, 31 (1992) L853-L855.

[4] S. H. Wei, A. Zunger, Physical Review Letters, 76 (1996) 664-667.

[5] K. Onabe, D. Aoki, J. Wu, H. Yaguchi, Y. Shiraki, Physica Status Solidi (a), 176 (1999) 231-235.

[6] H. Grüning, L. Chen, T. Hartmann, P. J. Klar, W. Heimbrodt, F. Höhnsdorf, J. Koch, W. Stolz, Physica Status Solidi (b), 215 (1999) 39-45.

[7] D. A. Clugston, P. A. Basore, PC1D version 5: 32-bit solar cell modelling on personal computers. Conference Record of the 26th IEEE Photovoltaic Specialists Conference, (1997) 207–210.

[8] The global standard spectrum (AM1.5g), https://www2.pvlighthouse.com.au/resources/courses/altermatt/The%20Solar%20Spectrum/The%20global%20standard%20spectrum%20(AM1-5g).aspx

[9] A. Biswas , B. S. Yadav , D. Bhattacharyya, N. K. Sahoo, S. S. Major, R. S. Srinivasa, Journal of Non-Crystalline Solids, 357 (2011) 3293–3300.

[10] G. F. Brown, J. W. Ager III, W. Walukiewicz, and J. Wu, Solar Energy Materials & Solar Cells, 94 (2010) 478-483.

[11] I. A. Ribeiro, F. J. Ribeiro, A. S. Martins, Solid State Communications, 186 (2014) 50–55.

[12] S. Adachi, Properties of Semiconductor Alloys: Group-IV, III–V and II–VI Semiconductors, Wiley: New York, (2009).

[13] R. Quay, Gallium Nitride electronics, Springer Series in Materials Science, Springer, (2008).

[14] M. Levinstein, S. Rumyantsev and M. Shur, Handbook Series on Semiconductor Parameters, vol. 1, 2, World Scientific, London, (1996), (1999).

[15] S. W. Koch, Microscopic Theory of Semiconductors: Quantum Kinetics, Confinement and Lasers, 212, World Scientific, (1995).

[16] H. Mathieu, Physique des semiconducteurs et des composants électroniques, 5ème édition Dunod (2001).

[17] K.N. Riaz, H. Ullah, S. Khalid, A.S. Malik, E. Ahmed, Journal of Faculty of Engineering & Technology, 23(1) (2016) 25-31.

[18] H. Okumura, S. Yoshida, and T. Okahisa, Applied Physics Letters, 64 (1994) 2997–2999.

[19] https://fr.scribd.com/document/98540290/Gan-Band-Str

[20] J. G. Kim, A. C. Frenkel, H. Liu and R. M. Park, Applied Physics Letters, 65 (1994) 91-93.

[21] J. R. L. Fernandez, V. A. Chitta, E. Abramof, A. Ferreira da Silva, J. R. Leite, A. Tabata, D. J. As, T. Frey, D. Schikora, and L. Lischka, (in: GaN and Related Alloys - 1999. Symposium (Materials Research Society Symposium Proceedings Vol. 595); Warrendale, PA, USA: Mater. Res. Soc, (2000).

[22] M. Suzuki, T. Uenoyama, Solid-States Electronics 41 (1997) 271-274.

[23] N. Miyashita, Y. Shimizu, N. Kobayashi, Y. Okada, M. Yamaguchi, Conference Record of the 2006 IEEE 4th World Conference on, IEEE, (2006).

[24] A. Aho, A. Tukiainen, V. Korpijärvi, V. Polojärvi, AIP Conference Proceedings, Toledo, Spain (2012).

[25] B. M. Kayes, H. Nie, R. Twist, S. G. Spruytte, F. Reinhardt, I. C. Kizilyalli, and G.S. Higashi, Photovoltaic Specialists Conference (PVSC), 2011 37th IEEE, Seattle, WA, (2011).